

Electrochemical Reforming of Glycerol in Alkaline PBI-Based PEM Reactor for Hydrogen Production

Joanna de Paula^a, Deborah Nascimento^a, José J. Linares^a

^aInstituto de Química, Universidade de Brasília, Campus Darcy Ribeiro CP 4478 70910-900, Brasília, Distrito Federal, Brazil
 joselinares@unb.br

One possible route for glycerol utilisation is through a reforming process in which clean hydrogen can be produced. This study presents the results of an Alkaline Membrane Electroreforming Reactor operated with KOH-doped polybenzimidazole (PBI). Commercial PtRu/C and Pt/C are used as catalysts for the anode and the cathode, respectively. The influence of two important operating variables, the temperature, and the composition of the cathode feed solution is studied. A significant enhancement in the cell performance is observed with the temperature until 90°C. The highest efficiency for H₂ production (comparison with the amount predicted from Faraday's law) corresponds to a KOH concentration in the cathode feed solution of 2 mol L⁻¹. Logically, higher current densities favours the amount of hydrogen produced and approaches the experimental values to the theoretical ones. Finally, the analyses of the product distribution show that more oxidized species can be obtained the higher the temperature and the current density, though the main products are C₃ organic acids, especially tartronic acid.

1. Introduction

The glycerol reforming process has been widely studied over the last decades, involving heterogeneous catalysts (Ni, Co, Inconel 625 Alloy, Ni-Mg-Al, etc.) on different supports (perovskites, alumina, ceria, titania, lanthanum oxide, etc.) (Dou et al., 2014; Markočič et al, 2013) and operating conditions (temperature, supercritical water, sorption enhancement, operating mode for minimizing deactivation processes). Relevant steps have been given in order to obtain efficient system for supplying hydrogen.

Hydrogen is considered the best energy vector in the near future. Its usage offers some advantages, such as cleanness in its combustion process and the largest energy density. However, hydrogen presents the well-known shortcoming of its absence as natural resource in the earth. Hence, hydrogen needs to be produced by "lysis" processes of organic molecule, mainly through steam reformat or gasification (syngas), or water electrolysis (Bolat and Thiel, 2014). Electrolysis processes are gaining interest in the last few years, due to the possibility of producing pure hydrogen. However, this process consumes a large amount of energy in order to overcome the large overpotentials, especially in the case of the water oxidation. Also, due to the high anode overpotentials, the variety of electrode materials is very limited. One possible alternative to water electrolysis is an alcohol electrolysis process. The high energy contained in these fuels supplies part of the requirements, reducing the external demand. More interestingly, if a bioalcohol is used, the process can be considered as environmentally friendly. Very promising results have been already presented in the literature. Studies focused on ethanol and bioethanol electrochemical reforming (also known as electro-reforming) were presented by Caravaca et al. (2012, 2013) and Lamy et al. (2014), on glycerol by Kongjao et al. (2011) and Marshall and Haverkamp (2008), on methanol by Sasikumar et al. (2008) and formic acid by Lamy et al. (2012).

Given these antecedents, this study intends to investigate the possibility of implementation of a glycerol electro-reforming in an alkaline Polymer Electrolyte Membrane reactor based on the use of KOH-doped Polybenzimidazole (PBI). The usage of an alkaline environment presents the advantage of an improved glycerol electrooxidation kinetics. Furthermore, glycerol can be oxidized to several larger added value

products, such as mesoxalic, tartronic and glyceric acid, raw materials for the pharmaceutical industry (Zhang et al., 2012). Thus, the electrochemical production of hydrogen has been assessed for different temperatures, current densities and compositions of the cathodic solution, in order to understand the behavior of the system under different operating conditions. In addition, the products distribution obtained from the glycerol electrooxidation has been quantified by HPLC analyses.

2. Experimental

2.1 Preparation of the membrane-electrode-assembly (MEA)

Commercial bimetallic PtRu/C and Pt/C (20% metal on carbon, atomic ration 1:1 in the bimetallic material, BASF Fuel Cells) were used as anode and cathode catalysts, respectively. The catalytic inks were prepared by mixing the necessary amounts of the catalysts powders and 10% wt. Nafion[®] referred to the amount of carbon in the catalysts (from an original solution of 5% in a mixture of aliphatic alcohols) in isopropanol until obtaining a slurry. This was ultrasonicated for 5 minutes and left to evaporate in order to guarantee the expected agglutinating effect of Nafion on the carbon particles. Next, few drops of isopropanol were added in order to form a thick slurry, which was applied by brushing onto a home-made gas diffusion layer (Carbon Cloth + microporous layer containing 3 mg cm⁻² + 15 % Teflon). The active area of the electrodes was 4 cm², with a metal loading in the anode of 2 mg cm⁻² and 1 mg cm⁻² in the cathode. The electrodes were dried for 1 hour in an oven at 80°C. The anion conducting membrane was a KOH doped PBI (immersed in 6 mol L⁻¹, PBI membrane kindly donated by Danish Power System, Dapossy), with an approximate thickness of 60 µm. A piece slightly larger than the electrode size was cut, superficially blotted with filter paper and placed between the electrodes. No hot-pressing was applied for forming the MEA.

2.2 Structural and morphological characterisation

Previous to the fuel cell tests, the two catalysts were briefly characterized by X-ray Diffraction from 20 to 80 ° (0.05 ° step, 0.5 ° min⁻¹) in a D8 Focus (Rigaku Corp., Japan). Transmission electron images (TEM) were recorded on a Philips CM-120 microscope operating at 120 kV. The actual composition of the bimetallic catalyst was confirmed by Energy Dispersive X-Ray Spectrometer (EDS) in a Zeiss-Leica/440 SEM microscope.

2.3 Electrochemical tests

The electrochemical performance of the system was evaluated by using a classical Proton Exchange Membrane Fuel Cells single unit. It consists of two graphite monopolar plates with parallel channels (1 mm thick and deep) containing the voltage probes. These plates are supported by two stainless steel (AISI 316) plates onto which the current probes were drilled. The temperature was controlled by a temperature controller (Novus N1020). The necessary heat was delivered by heating rods inserted in the stainless steel plates. A peristaltic pump (Milan BP-200) was used for pumping the different solutions, with a flow rate of 1 mL min⁻¹. Different catholytes were tested: water, 1, 2 and 4 mol L⁻¹ KOH, whereas the anolyte was 1 mol L⁻¹ glycerol and 4 mol L⁻¹ KOH (Nascimento and Linares, 2014).

The electrochemical measurements were carried out on a Potentiostat/Galvanostat PGSTAT302 (Metrohm Autolab). The polarization curves were recorded by linear sweep voltammetry at a scan rate of 0.5 mV s⁻¹. For the assessment of the hydrogen production and efficiency the system was operated in galvanostatic mode, in order to control strictly the current and, therefore, facilitate the estimation of those parameters. Hydrogen evolved in the cathode was collected on an inverted burette. Comparison between the experimental H₂ collected and the Faraday's law prediction gave rise to the calculation of the efficiency.

2.4 Product distribution

In order to determine the glycerol electrooxidation products distribution, HPLC injections were carried out, taking a 2 mL sample of the solution going in and coming out the cell. In order to separate the different products, an ion exchange chromatographic column (Polypore-H, Perkin Elmer, 22 cm × 4.6 mm, 10 µm) was used. The mobile phase was 0.025 mol L⁻¹ H₂SO₄ at room temperature with a flow rate of 0.075 mL min⁻¹. A 5 µL sample was injected into the column. Each compound was identified by comparison with the standards (glycerol, glyceric acid, glycolic acid, oxalic acid, tartronic acid, mesoxalic acid, glyoxilic acid, lactic, formic acid, glyceraldehyde and dihydroxyacetone). Due to the difficult separation, and in order to confirm each peak, successive preparation of samples containing one additional standard (in growing time sequence) were injected. A PDA detector was used at different wavelength (190, 210, 225, 240 and 250 nm). The chromatograms of the effluent and affluent solutions were compared in order to identify the products electrogenerated.

3. Results and discussion

3.1 Structural and morphological characterisation

Previous to the glycerol electro-reforming experiments, the two catalysts used in this study were morphological and structurally characterized. Figure 1 shows the XRD diffractograms of the two catalysts and the corresponding TEM images.

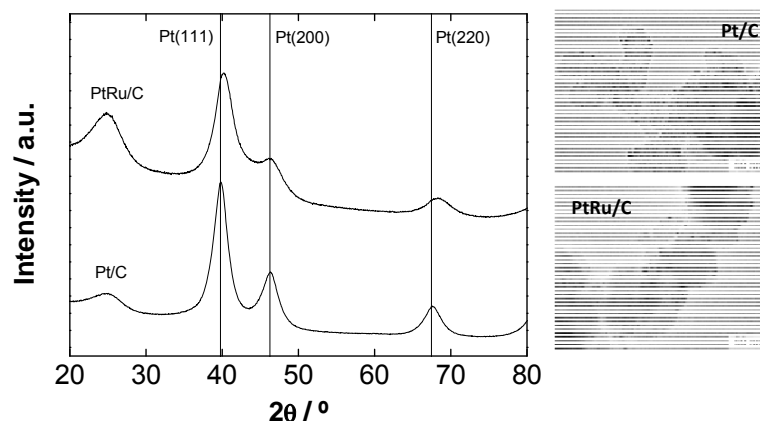


Figure 1. XRD patterns and TEM images of the PtRu/C and Pt/C catalysts used in this study

As it can be observed, the Pt/C and PtRu/C catalysts show the typical peaks associated to the Pt fcc crystalline structure. However, in the case of the PtRu/C, there is a slight shift of the peaks to larger angle values. This is due to the insertion of some Ru atoms to the Pt crystalline lattice (PtRu alloy). A simple calculation by applying the Vegard's law (Linares et al., 2013) allows for estimating the alloy degree of the PtRu/C. Moreover, Scherrer's equation can be applied to the Pt(220) diffraction peak in order to estimate the crystal size. The average particle size was estimated from the TEM images with the aid of an image processing software. It is possible to observe that both catalysts show metal particles in the nanometric range spread onto the carbon support. The values of these parameters, along with the actual composition of the catalysts from EDS analyses are collected in Table 1.

Table 1: Main information from the XRD patterns, TEM images and EDS analysis

Catalyst	Actual composition	Crystal size / nm	TEM average particle size	Alloy fraction
Pt/C	-	3.4	2.8	-
Pt ₁ Ru ₁ /C	Pt ₁ Ru _{1.3} /C	2.4	2.5	0.39

Values in Table 1 confirm that the two materials are in the nanometric range, with a slight enrichment of the bimetallic PtRu/C compared to the 1:1 expected atomic ratio. Finally, 39% of the Ru included in the bimetallic catalyst is actually inserted within the crystalline Pt lattice.

3.2 Single cell glycerol electro-reforming tests

a) Influence of the temperature

The temperature exerts a significant effect on the electrochemical systems. All the processes occurring in the systems significantly get promoted: catalyst activity, membrane conductivity and mass diffusion in the gas diffusion and catalytic layer (Miller and Bazilak, 2011). Figure 2 shows the results corresponding to the effect of the temperature of the glycerol electro-reforming process. The anolyte was 4 mol L⁻¹ KOH and 1 mol L⁻¹ glycerol, whereas the catholyte used in this system was water. As expected, the increase in the temperature brings a significant improvement in the current density (and hence, hydrogen production). On the other hand, in terms of hydrogen generation, it can be observed that the higher the current density, the larger is the amount of hydrogen produced, even though high current densities can be only obtained at the highest temperature (90°C). Figure 2c displays some interesting results. The efficiency for hydrogen production increases with the current density. Although this needs to be more deeply analysed, one possible reason lies on the crossover of hydrogen from the cathode to the anode, whose effect is more evident at low current densities (low hydrogen production rates). This becomes even clearer analysing the effect of the temperature on the efficiency for a certain current density. As observed, there is a slight

decrease in the efficiency, due to the higher crossover at higher operating temperatures (Nunes Couto and Linares, 2014).

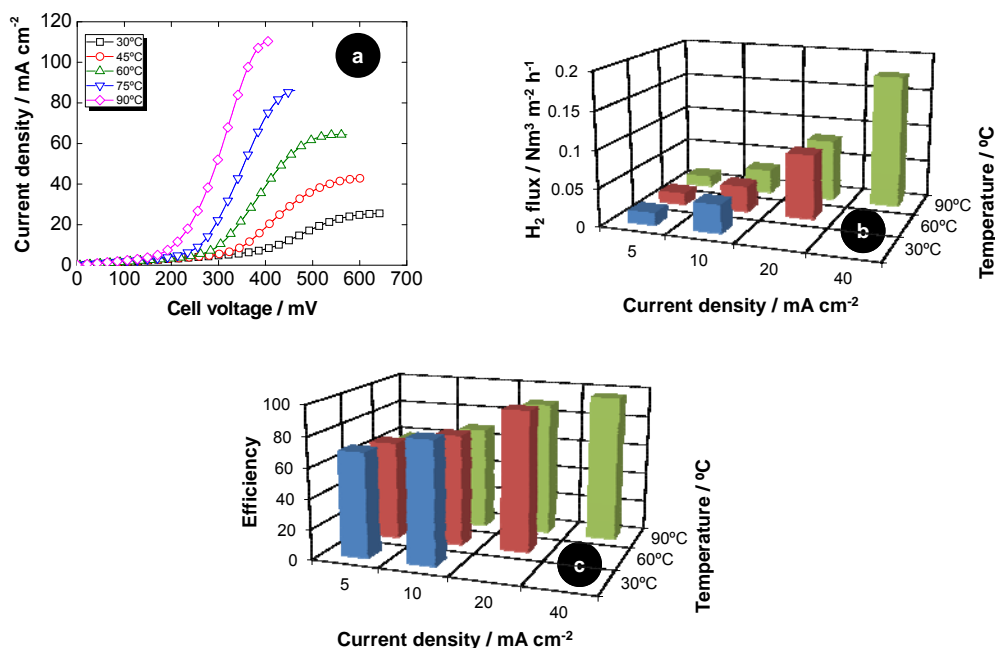


Figure 2. (a) Polarization curves of the glycerol electro-reforming system, (b) Hydrogen produced at different temperatures and current densities, and (c) Hydrogen production efficiency compared to Faraday's law (water was fed into the cathode)

b) Influence of the concentration of the cathodic solution

Taking into account that the cathode reaction for hydrogen evolution in the cathode requires of water and OH⁻ species are generated ($2\text{H}_2\text{O} + 2\text{e}^- \rightarrow \text{H}_2 + 2\text{OH}^-$), different feed solutions were studied, from ultrapure water to different KOH concentrations (1, 2 and 4 mol L⁻¹). Figure 3 shows the results of the different KOH concentration. As it can be seen, there is an optimum in the KOH concentration. From pure water to 2 mol L⁻¹, the current density (and hence, the hydrogen production, see Figure 3b) increases, especially at high current densities. One possible reason for this behaviour is the expected enhanced OH⁻ transportation in the KOH-doped membrane and in the electrode the higher is the KOH concentration (Nascimento and Linares, 2014). Indeed, PBI by itself is not an anionic exchange material, but it possesses the ability of absorbing KOH molecules within its structure (Hou et al., 2008). In the case of feeding a 4 mol L⁻¹ KOH solution to the cathode, one significant feature is the reduction of the efficiency for the hydrogen production. As reported by Qi et al. (2013), a high KOH concentration could result in a large OH coverage of the Pt active sites, impeding the water reduction. Finally, the hydrogen (and very likely also the glycerol) crossover seems to be promoted at the highest KOH as reflected by the own reduction of the efficiency.

c) Product distribution

Finally, product distributions obtained from the glycerol electrooxidation process was quantified by HPLC. The percentage of the main detected products is shown in Figure 4. As it can be seen in Figure 4a, the increase in the current density favours the production of more oxidized products (increase in the tartronate percentage vs. glycerate one) and also allows for obtaining more oxidized C₂ products (more oxalate compared to glycolate), due to the higher energy available for breaking the C-C bonds and more oxygenated groups in the catalyst surface (Zhang et al., 2012). On the other hand, Figure 4b shows that an increase in the temperature, and therefore, in the energy available for the electrochemical reaction, leads to a higher C₂ products percentage, especially visible at 90°C, with the appearance of significant amounts of oxalate, and even a small amount of formiate (C₁ product). At 60°C, the main C₂ product is glycolate, whereas at 30°C the most significant products are mainly tartronate and glycerate.

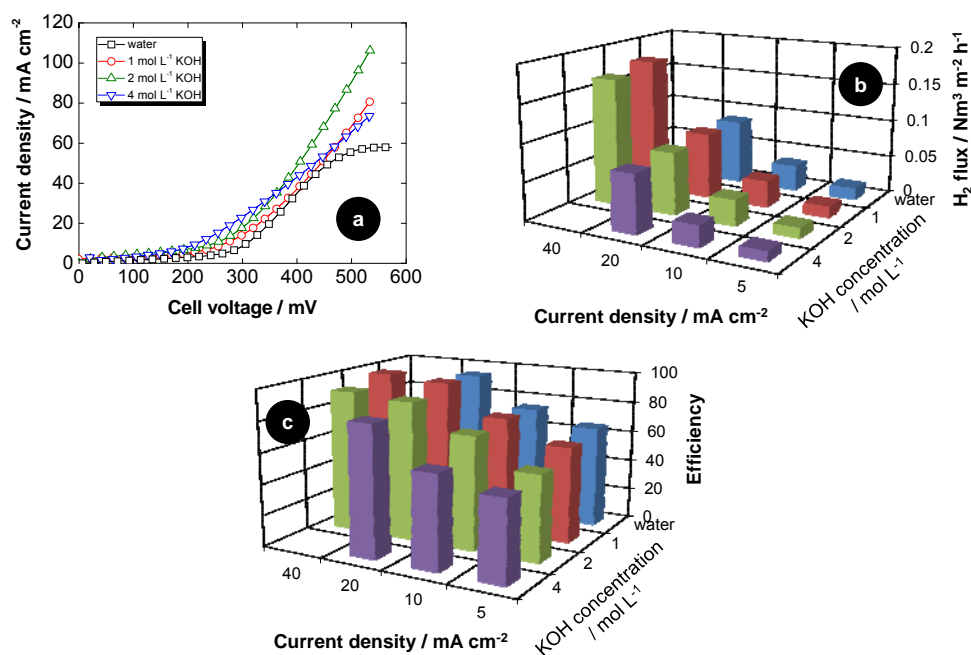


Figure 3. (a) Polarization curves of the glycerol electro-reforming system, (b) Hydrogen produced at different KOH concentration in the catholyte and current densities, and (c) Hydrogen production efficiency compared to Faraday's law (operating temperature of 60°C)

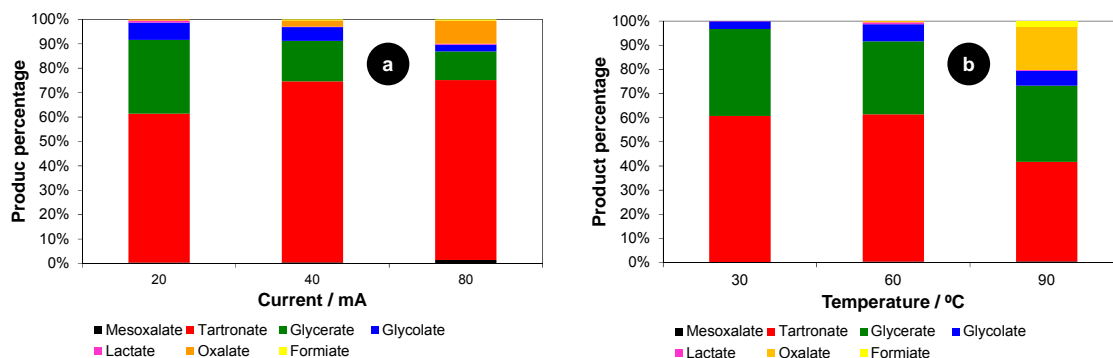


Figure 4. (a) Product distribution at 60°C for different currents, (b) Product distribution for different temperatures at a current of 20 mA

4. Conclusions

This study has demonstrated the possibility of producing hydrogen from a glycerol-electroreforming process. The highest hydrogen production can be achieved at the highest current densities and temperatures (up to 90°C), feeding the cathode with a 2 mol L⁻¹ KOH solution. However, in the case of the hydrogen efficiency production, the best conditions corresponds to high current densities at an intermediate temperatures (60°C), in order to minimise the crossover effects, with the same KOH concentration for the catholyte. On the other hand, added value products can be obtained from the glycerol electrooxidation in the anode, being the C₃ organic acids the most abundant ones, especially tartronate, although higher temperatures and current densities favour the most oxidized C₂ products (glycolate and especially oxalate), making attractive this alternative for hydrogen and organic acids derived of glycerol production,

Acknowledgements

The authors want to thank the Conselho Nacional de Desenvolvimento Científico e Tecnológico (CNPq) for the financial support through the project (Universal Call 474381/2013-7). Also, Dr. Sabrina Zignani (ITAE, Italy) and Mr. Thairo Araujo (IQSC, USP, Brazil) are acknowledged for obtaining of the TEM images and EDS analyses, respectively.

References

- Bolat, P., Thiel, C., 2014, Hydrogen supply chain architecture for bottom-up energy systems models. Part 2: Techno-economic inputs for hydrogen production pathways, *Int. J. Hydrogen Energy*, in press.
- Caravaca, A., Sapountzi, F.M., De Lucas-Consuegra, A., Molina-Mora, C., Dorado, F., Valverde, J.L., 2012, Electrochemical reforming of ethanol-water solutions for pure H₂ production in a PEM electrolysis cell, *Int. J. Hydrogen Energy*, 37, 9504-9513.
- Caravaca, A., De Lucas-Consuegra, A., Calcerrada, A.B., Lobato, J., Valverde, J.L., Dorado, F., 2013, From biomass to pure hydrogen: Electrochemical reforming of bio-ethanol in a PEM electrolyser, *Appl. Catal. B-Environ.*, 134-135, 302-309.
- Dou, B., Song, Y., Wang, C., Chen, H., Xu, Y., 2014, Hydrogen production from catalytic steam reforming of biodiesel byproduct glycerol: Issues and challenges, *Renew. Sust. Energ. Rev.*, 30, 950-960.
- Hou, H., Sun, G., He, R., Sun, B., Jin, W., Liu, H., Xin, Q., 2008, Alkali doped polybenzimidazole membrane for alkaline direct methanol fuel cell, *Int. J. Hydrogen Energy*, 33, 7172-7176.
- Kongjao, S., Damronglerd, S., Hunsom, M., 2011, Electrochemical reforming of an acidic aqueous glycerol solution on Pt electrodes, *J. Appl. Electrochem*, 41, 215-222.
- Lamy, C., Devadas, A., Simoes, M., Coutanceau, C., 2012, Clean hydrogen generation through the electrocatalytic oxidation of formic acid in a Proton Exchange Membrane Electrolysis Cell (PEMEC), *Electrochim. Acta*, 60, 112-120.
- Lamy, C., Jaubert, T., Baranton, S., Coutanceau, C., 2014, Clean hydrogen generation through the electrocatalytic oxidation of ethanol in a Proton Exchange Membrane Electrolysis Cell (PEMEC): Effect of the nature and structure of the catalytic anode, *J. Power Sources*, 245, 927-936.
- Linares, J.J., Rocha, T.A., Zignani, S., Paganin, V.A., Gonzalez, E.R., 2013, Different anode catalyst for high temperature polybenzimidazole-based direct ethanol fuel cells, *Int. J. Hydrogen Energy*, 38, 620-630.
- Markočič, E., Kramberger, B., Van Bennekom, J.G., Jan Heeres, H., Vos, J., Knez, Ž., 2013, Glycerol reforming in supercritical water; A short review, *Renew. Sust. Energ. Rev.*, 23, 40-48.
- Marshall, A.T., Haverkamp, R.G., 2008, Production of hydrogen by the electrochemical reforming of glycerol-water solutions in a PEM electrolysis cell, *Int. J. Hydrogen Energy*, 33, 4649-4654.
- Miller, M., Bazylak, A., 2011, A review of polymer electrolyte membrane fuel cell stack testing, *J. Power Sources*, 196, 601-613.
- Nascimento, A.P., Linares, J.J., 2014, Performance of a direct glycerol fuel cell using KOH doped polybenzimidazole as electrolyte, *J. Braz. Chem. Soc.*, 25, 509-516.
- Nunes Couto, R., Linares, J.J., 2014, Caracterização físico-química e desempenho eletroquímico das membranas de polibencimidazol impregnadas com KOH como eletrólito para células a combustível de álcool direto alcalinas, Extended abstract submitted to the Brazilian Congress of Chemical Engineering.
- Qi, J., Xin, L., Zhang, Z., Sun, K., He, H., Wang, F., Chadderton, D., Qiu, Y., Liang, C., Li, W., 2013, Surface dealloyed PtCo nanoparticles supported on carbon nanotube: Facile synthesis and promising application for anion exchange membrane direct crude glycerol fuel cell, *Green Chem.*, 15, 1133-1137.
- Sasikumar, G., Muthumeenal, A., Pethaiah, S.S., Nachiappan, N., Balaji, R., 2008, Aqueous methanol eletrolysis using proton conducting membrane for hydrogen production, *Int. J. Hydrogen Energy*, 33, 5905-5910.
- Zhang, Z., Xin, L., Li, W., 2012, Electrocatalytic oxidation of glycerol on Pt/C in anion-exchange membrane fuel cell: Cogeneration of electricity and valuable chemicals, *Appl. Catal. B-Environ.*, 119-120, 40-48.